polysaccharides

MDPI

Article

Biopolymer from *Annona muricata* Residues as a Potential Sustainable Raw Material for Industrial Applications

Igor F. S. Ramos [1], Samuel C. Dias [1], Talissa B. C. Lopes [1], Francisco T. dos S. Silva Júnior [2], Ricardo de Araújo [1], Stanley J. C. Gutierrez [2], Claudia Pessoa [3], Josy A. Osajima [1], Marcia S. Rizzo [1], Edson C. Silva-Filho [1], Manuela Amorim [4], Óscar Ramos [4], Alessandra B. Ribeiro [4,*] and Marcilia P. Costa [1,*]

[1] Interdisciplinary Laboratory for Advanced Materials (LIMAV), Materials Science and Engineering Graduate Program (PPGCM), Federal University of Piauí, Teresina 64049-550, PI, Brazil; igor.ramos@ufpi.edu.br (I.F.S.R.); samuel.c.dias@hotmail.com (S.C.D.); talissa.brenda@gmail.com (T.B.C.L.); ricardodearaujo@ufpi.edu.br (R.d.A.); josyosajima@ufpi.edu.br (J.A.O.); marciarizzo@ufpi.edu.br (M.S.R.); edsonfilho@ufpi.edu.br (E.C.S.-F.)

[2] Department of Pharmacy, Federal University of Piauí, Teresina 64049-550, PI, Brazil; franciscotiago_10@outlook.com (F.T.d.S.S.J.); stanleychavez@ufpi.edu.br (S.J.C.G.)

[3] Drug Research and Development Center, Federal University of Ceará, Fortaleza 60430-270, CE, Brazil; cpessoa@ufc.br

[4] CBQF—Centro de Biotecnologia e Química Fina—Laboratório Associado, Escola Superior de Biotecnologia, Universidade Católica Portuguesa, Rua Diogo Botelho 1327, 4169-005 Porto, Portugal; mamorin@ucp.pt (M.A.); oramos@ucp.pt (Ó.R.)

* Correspondence: abribeiro@ucp.pt (A.B.R.); marciliapc@ufpi.edu.br (M.P.C.)

Abstract: *Annona muricata* is a fruit species belonging to the Annonaceae family, which is native to the warmer tropical areas of North and South America. A large amount of discarded residue from *A. muricata* is of interest for obtaining new industrial inputs. To propose the applications of the biopolymer from *A. muricata* residues (Biop_AmRs), this study aimed to characterize this input chemically and functionally, as well as to evaluate its potential for hemocompatibility and cytotoxicity activity in vitro. Biop_AmRs is an anionic heteropolysaccharide composed of glucose, arabinose, xylose, galactose, mannose, uronic acid, and proteins. This biopolymer exhibited a semicrystalline structure and good thermal stability. Biop_AmRs exhibited excellent water holding capacity, emulsifying properties, and mucoadhesiviness and demonstrated hemocompatibility and cytocompatibility on the L929 cell line. These results indicate possible applications for this biopolymer as a potential environmentally friendly raw material in the food, pharmaceutical, biomedical, and cosmetic industries.

Keywords: Annonaceae; polysaccharide; vegetable residues; industrial waste

Citation: Ramos, I.F.S.; Dias, S.C.; Lopes, T.B.C.; Silva Júnior, F.T.d.S.; de Araújo, R.; Gutierrez, S.J.C.; Pessoa, C.; Osajima, J.A.; Rizzo, M.S.; Silva-Filho, E.C.; et al. Biopolymer from *Annona muricata* Residues as a Potential Sustainable Raw Material for Industrial Applications. *Polysaccharides* **2024**, *5*, 523–539. https://doi.org/10.3390/polysaccharides5040033

Academic Editors: Karin Stana Kleinschek, Valentina Siracusa, Nadia Lotti, Michelina Soccio and Alexey L. Iordanskii

Received: 26 June 2024
Revised: 1 August 2024
Accepted: 20 September 2024
Published: 26 September 2024

1. Introduction

Soursop (*Annona muricata* L.) is an important tropical fruit of the Annonaceae family. It is native to the Americas and the Caribbean [1]. The fruits have a sweet white pulp containing numerous small seeds. The majority of the fruit, approximately 80%, is composed of water, carbohydrates, and non-reducing sugars [2,3]. A study conducted by Lopes Leivas et al. (2023) [4] identified the presence of several polysaccharides, including homogalacturonan, type II arabinogalactan, arabinan-rich pectin, acid xylan, and a xylan-xyloglucan complex, in the pulp of *A. muricata* fruits. This fruit also contains a variety of constituents, including vitamins, amino acids, phenolic compounds, flavonoids, carotenoids, saponins, and acetogenins [1]. Soursop is widely consumed and is commercially important in several countries around the world, and its production and processing generate a significant amount of waste [5].

Food waste can be generated at any level along the food production chain, including harvesting, processing, and manufacturing [6]. Currently, many tropical fruits are traded

around the world due to increasing demand. In 2018, 7.1 million tons of tropical fruits were consumed globally, and the cultivation of fruits for commercialization has increased [7]. As a result, this increase in food supply to meet the demands of a growing population has led to an increase in these food residues [8].

Among these plant residues, we highlight the polysaccharides, natural polymers, or biopolymers found in the components of plant cell walls [9]. These macromolecules are versatile in their biological properties and technological applications [9,10]. These plant derivatives have also attracted research interest due to their biocompatibility, biodegradability, and low toxicity [11].

Several studies have shown that plant polysaccharides possess unique physicochemical properties, such as high average water absorption capacity and the formation of viscous colloidal dispersions [12,13]. These properties increase the potential use of these inputs. Polysaccharides have a variety of applications in the food sector, in which they can be used to make or coat foods or to create food packaging. In the biomedical and pharmaceutical sectors, they are employed in the obtention of nanoparticles, scaffolds, transdermal patches, dressings, and different forms of drug carriers. Finally, in the cosmetics sector, polysaccharides are used in gels, creams, and other similar products [13–16].

Therefore, there is a growing interest in using green chemistry principles and environmentally friendly inputs to develop new materials and products using natural resources that may be harmful to the environment [17]. Thus, this work aims to show the importance of exploring an alternative and eco-friendly input derived from A. muricata fruit waste. Numerous studies have investigated the chemical and physicochemical properties of the soursop pulp; however, the residues have been relatively understudied.

In this context, this study aimed to evaluate the properties of the biopolymers from *A. muricata* fruit residues (Biop_AmRs). The considerable quantity of *A. muricata* fruit waste has great potential for industrial use, and in this work, we sought to investigate the innovative properties of the biopolymer. The initial stage of this study evaluated the chemical and functional characteristics of the biopolymer. The mucoadhesive potential of the biopolymer was evaluated to ascertain its suitability for use in orodispersible drug release forms. Finally, cyto- and hemocompatibility tests were conducted to assess the safety of biopolymers in biomedical and pharmaceutical devices.

2. Materials and Methods

2.1. Chemicals and Reagents

Annona muricata residues (Biop_AmRs) were obtained from a local fruit pulp manufacturer. Sodium alginate was purchased from Êxodo Científica (98.4%) (Sumaré, SP, Brazil). Guar gum (*Cyamopsis tetragonoloba*) was obtained from SM Empreendimentos Farmacêuticos Ltda (99.9%) (São Paulo, SP, Brazil). The RPMI 1640 medium, penicillin, and streptomycin, all sterile and suitable for cell culture, were purchased from Gibco (Invitrogen, Carlsbad, CA, USA). Fetal bovine serum, sterile and for cell culture, was purchased from Cultilab (Campinas, SP, Brazil). Sheep blood agar plates were bought at Laborclin (LB Laborclin, Pinhais, PR, Brazil). Mueller–Hinton broth and casein soy broth were obtained from Merck® (Merck & Co., Inc., Rahway, NJ, USA), and brain–heart infusion broth was obtained from Kasvi (Kasvi®, São José do Pinhais, PR, Brazil). All other chemicals used were analytical grade and used as indicated by their manufacturers.

2.2. Extraction of Biopolymer from A. muricata Residues

The polysaccharide was extracted from *A. muricata* residues (Biop_AmRs) without seeds, according to previously published methods, with adaptations [18]. Initially, 20.0 g of Biop_AmRs was homogenized in 300 mL of distilled water at 80 °C under constant stirring (680 rpm) for 30 min. Subsequently, 300 mL of heated distilled water at 80 °C was added to the mixture. The obtained ratio of Biop_AmRs and distilled water was 1:30 (w/v). The mixture was heated (80 °C) and subjected to constant stirring (1330 rpm) for

30 min. Thereafter, the mixture was precipitated twice in absolute ethanol (1:2, v/v) and vacuum-filtered. The residue was dried at 50 °C for 24 h.

2.3. Biop_AmRs Characterizations

2.3.1. pH, Conductivity, and Zeta Potential (ζ)

The pH and conductivity were determined at 25 °C in a PHS3BW BEL instrument (Bel Engineering®, Monza, MB, Italy) using 1 wt% Biop_AmRs solution. The zeta potential (ζ) was measured in a Zetasizer Nano-ZS90 (Malvern Instruments, Malvern, UK) at 25 °C, for the dispersion of Biop_AmRs at a concentration of 0.1 wt% prepared in water obtained from the Milli-Q water purification system (Millipore Corp., Bedford, MA, USA), and readings were taken in triplicate after five minutes of equilibration.

2.3.2. Molecular Weight

The molecular weight of the Biop_AmRs was evaluated through a chromatographic analysis in an Agilent 1260 Infinity II LC System chromatograph (Agilent Technologies Inc., Santa Clara, CA, USA) equipped with an Agilent 1290 Infinity II Evaporative Light Scattering Detector, PL aquagel-OH MIXED-M, and aquagel-OH 20 columns. Samples were prepared in 10 mM of ammonium acetate and filtered. The system was calibrated with Shodex standards Waters Chromatography (Waters™, Madrid, Spain). All chromatograms were analyzed using the Agilent OpenLAB CDS ChemStation software (1.12.3.1008).

2.3.3. Analysis of the Monosaccharide Composition

The method for the analysis of the monosaccharide composition of the Biop_AmRs was described by Coelho et al. [19]. The biopolymer was prehydrolyzed in 0.2 mL of 72% H_2SO_4 for 3 h at 25 °C, followed by hydrolysis for 2.5 h in 1 mol L^{-1} of H_2SO_4 at 100 °C. An Agilent 7890B gas chromatograph (GC) system (Agilent Technologies Inc., Santa Clara, CA, USA) with a split/splitless capillary inlet and flame ionization detector (FID) was used in this study. A column DB-225 capillary column 30 m in length, 0.25 mm in diameter, an 0.15 μm in thickness was utilized in the equipment. 2-deoxyglucose was used as an internal standard.

2.3.4. Protein Content

The protein content based on the determination of nitrogen was carried out according to the Dumas method [20]. A total of 150 mg of Biop_AmRs was weighed in an aluminum crucible and examined on the Dumatec™ 8000 equipment (Foss, Hillerød, Denmark). The experimental conditions were as follows: the flow rate was 195.0 mL min^{-1}, and the oxygen flow rate was 400 mL min^{-1}, with a pressure of 1200 mBar. The protein content was calculated based on the total nitrogen content. This was multiplied by the conversion factor of 6.25. Ethylenediaminetetraacetic acid (EDTA) was used as a standard for constructing the nitrogen calibration curve (10.9–150.2 mg).

2.3.5. Fourier Transform Infrared Spectroscopy (FTIR)

The spectra were achieved on the Spectrum 400 spectrophotometer (PerkinElmer™, Waltham, MA, USA) using potassium bromide (KBr) disks of 5 mm in diameter. KBr disks with 500 mg of KBr powder and 5 mg of the sample were obtained using a bench punch machine. The background spectrum was measured against a pure KBr disk. The spectra of the polysaccharide sample were measured in the solid state and recorded in the range of 4000–500 cm^{-1}, with 64 scans at a resolution of 4 cm^{-1}.

2.3.6. X-ray Diffraction (XRD)

The analyses were carried out at room temperature in an XRD-6000 X-ray diffractometer (Shimadzu™, Kyoto, Japan) using copper Kα radiation (1.5418 Å), with a scan voltage of 40 kV and scan current of 30 mA. The Biop_AmRs sample was examined at a 2θ angle ranging from 5.0 to 75.0 degrees at a speed of 2° min^{-1}.

2.3.7. Thermogravimetric Analysis (TGA) and Derivative Thermogravimetry (DTG)

The thermal profile by thermogravimetric analysis (TGA) and differential scanning calorimetry (DSC) was performed using a Shimadzu thermogravimetric analyzer (Shimadzu™, Kyoto, Japan), model TGA-60, and DSC-60 under a nitrogen atmosphere (50 mL min^{-1}). For the scan, the samples were weighed in alumina pans (mass of 5 mg), and the temperature was raised to 600 °C, with a heating rate of 10 °C min^{-1}.

2.3.8. Scanning Electron Microscopy (SEM)

The Biop_AmRs sample was mounted on aluminum support and covered with Au in a Q150R deposition equipment (Quorum Technologies Ltd., Lewes, UK) for 30 s at 20 mA using atmospheric argon plasma. Then, the morphological characteristics of the sample were observed using scanning electron microscopy (SEM) through a Quanta FEG 250—FEI™ electron microscope (FEI Company, Hillsboro, OR, USA) with an acceleration voltage from 1 to 30 kV. The images were recorded digitally in variable magnifications of 1000 to 50,000×.

2.3.9. Technological Properties

The analyses of the functional properties of the Biop_AmRs were carried out according to methodologies described by Alpizar-Reyes et al. [21], with adaptations. The functional properties determined were water holding capacity (WHC), emulsifying ability (EA), emulsion stabilization (ES), foam index (FI), foam stability (FS), and film-forming ability. All analyses were performed in triplicate.

Water Holding Capacity (*WHC*)

A colloidal dispersion of 3 wt% of Biop_AmRs was prepared in distilled water and placed in previously weighed centrifuge tubes. Next, the dispersion was centrifuged for 15 min at 1600 rpm. The supernatant was discarded, and the sample was reweighed. The *WHC* was determined using Equation (1), as follows:

$$WHC\ (\%) = \frac{Sample\ mass\ after\ water\ absorption}{Dry\ sample\ mass} \times 100 \quad (1)$$

Emulsifying Ability (*EA*) and Emulsifying Stability (*ES*)

The emulsions were formulated by homogenizing 10 mL of a 3 wt% Biop_AmRs solution with 2.5 mL of soybean oil, maintaining the 1:4 ratio of oil: solution (v/v), in an Ultra-Turrax homogenizer (Ultra-Turrax, T50, IKA®, Staufen, Germany) at 6600 rpm for 3 min. The *EA* was calculated using Equation (2), as follows:

$$EA\ (\%) = \frac{Initial\ emulsion\ volume}{Total\ volume} \times 100 \quad (2)$$

After the homogenization step, the formulated emulsion remained at rest for 30 min. Then, the emulsion was centrifuged for 10 min at 1600 rpm. The emulsified layer was measured, and the *ES* was calculated using Equation (3), as follows:

$$ES\ (\%) = \frac{Final\ emulsion\ volume}{Initial\ emulsion\ volume} \times 100 \quad (3)$$

Foaming Ability (*FA*) and Foam Stability (*FS*)

A colloidal dispersion of 3 wt% of the Biop_AmRs was prepared. Then, the solution was stirred in an ultra-high-speed homogenizer (Ultra-Turrax, T50, IKA®, DE) at 6600 rpm for 5 min. The *FA* was calculated immediately after stirring (≅30 s), according to Equation (4), as follows:

$$FA\ (\%) = \frac{Initial\ foam\ volume}{Total\ suspension\ volume} \times 100 \quad (4)$$

Foam stability was calculated with the foam volume after 30 min of shaking using Equation (5), as follows:

$$FS\ (\%) = \frac{Final\ foam\ volume}{Total\ dispension\ volume} \times 100 \quad (5)$$

Film-Forming Ability

This analysis was performed according to the protocol of Davidović et al. [22], with adaptations. The film solution was prepared at 1 wt%, dissolving the powder of Biop_AmRs in distilled water, which was subjected to stirring until the sample was completely dispersed. Then, the glycerol plasticizer was added to a concentration of 3% (v/v), and the film-forming solution was cast in a silicone mold and dried at 50 °C.

2.3.10. Texturometric Analyses

Firmness, consistency, cohesiveness, and viscosity index parameters were analyzed using a TA-XT Plus texturometer (TA Instruments®, Surrey, UK). 100 g of the Biop_AmRs sample at 1 wt% concentration was analyzed on the equipment, with the probe (P/35 mm) introduced continuously at a velocity of 2.0 mm s^{-1}. Data were processed using the Exponent Lite 2009 software. The assay was performed in triplicate. Alginate and guar gum (*Cyamopsis tetragonoloba*), commercial biopolymers, were used as a sample for comparison.

2.3.11. Biological Assays

Ex Vivo Mucoadhesiveness

The mucoadhesion of Biop_AmRs to porcine oral mucosa was performed according to the method described by Ramos et al. [23]. All procedures were in accordance with the ethical principles established by the National Council for the Control of Animal Experiments (CONCEA) and the national legislation in force (Law No. 11,794 of 8 August 2008 and Law No. 9605 of 12 February 1998, Brazil). The ex vivo mucoadhesion method was performed on a TA.XT 2 Plus texturometer (TA Instruments, Surrey, UK) equipped with a load cell of 5 kg. The Biop_AmRs power was fixed in a probe (P/10). Prior to each new test, the porcine mucosa was moistened with a simulated saliva solution maintained at 37 °C. A force of 0.2 N was applied to the mucosa for 30 s at speeds of 0.5 mm s^{-1} (pre-test and test) and 5 mm s^{-1} (post-test). The result of the maximum detachment force (Fmax) required to separate the sample of the mucosa and the total amount of force involved in removing the sample of the mucosa (work of adhesion; Wad) were utilized to determine the mucoadhesive properties of the sample [24,25]. The peak displacement force (*PDF*) result was obtained using Equation (6).

$$PDF\ (N/cm^2) = \frac{F_0}{A_0} \quad (6)$$

where F_0 is the force required to detach the sample from the mucosa and A_0 is the area filled by the sample.

Cytocompatibility Assay

The cytocompatibility of the Biop_AmRs sample was achieved using the 3-[4,5-dimethylthiazol-2-yl]-2,5-diphenyltetrazolium (MTT) test according to the ISO 10993-5 standard [26]. The mouse fibroblast (L-929) cell line was used in this test. The cells were maintained in RPMI 1640 medium supplemented with 10% fetal bovine serum, 100 U mL^{-1} of penicillin, and 100 µg mL^{-1} of streptomycin at 37 °C, with 5% CO_2 and 95% atmospheric air. Briefly, 1×10^4 cells/100 µL of medium were distributed in 96-well plates. Biop_AmRs solutions, ranging from 62.5 to 500 µg mL^{-1}, were incubated with the cells. Doxorubicin (Doxo) was used as a positive control (0.1 µM). The absorbance of the samples was assessed using a microplate spectrophotometer (DTX800 Multimode Detector, Beckman Coulter, Brea, CA, USA) at 595 nm. The percentage of cell growth inhibition was calculated using

the following formula: (GI%) = [100 × (Sample Abs)/(Negative Control Abs)]. The tests were carried out in duplicates in three independent experiments. According to ISO 10993-5, a cell growth inhibition or reduction of cell viability by more than 30% is regarded as a cytotoxic effect.

Hemocompatibility Assay

Biop_AmRs was evaluated in a hemolytic activity test on sheep blood agar using the disk technique according to the methodology described by Kalegari et al. [27]. The sterile paper disks of 7 mm were impregnated with 50 µL of the sterile Biop_AmRs solution at a concentration of 1%, and, after drying, they were placed in the Petri dishes containing the blood agar. For the positive and negative controls, the disks were impregnated with 50 µL of Triton® X-100 (Merck & Co., Inc., Rahway, NJ, USA) and 50 µL of phosphate buffer, respectively. After applying the disks, the plates were incubated at 35 ± 2 °C for 24 h. After incubation, the hemolytic halos (mm) formed were evaluated.

2.3.12. Statistical Analysis

Data were expressed as mean ± standard deviation. A comparison of results from independent tests was analyzed using ANOVA, followed by Student's *t*-test, using the OriginPRO® Program. The cytocompatibility test was analyzed using ANOVA, followed by Dunnet's test to assess significance. In this study, we used a significance level of 5% ($p < 0.05$).

3. Results and Discussion

In the industrial processing of soursop, a large amount of waste is generated. The large amount of pulp residues aroused the interest of our research group in extracting and characterizing the biopolymer from *A. muricata* fruit residues (Biop_AmRs) contained in this sample.

3.1. Obtaining and Purification of Biop_AmRs

The Biop_AmRs obtained in the extraction can be seen in Figure 1. The biopolymer powder presented a yellowish color, no odor, and a fibrous appearance. A yield of 7.5% of Biop_AmRs was obtained after the extraction process. Ren et al. [28] extracted the crude polysaccharide from the fruit pulp of *Annona squamosa* and obtained a yield of 4.86%.

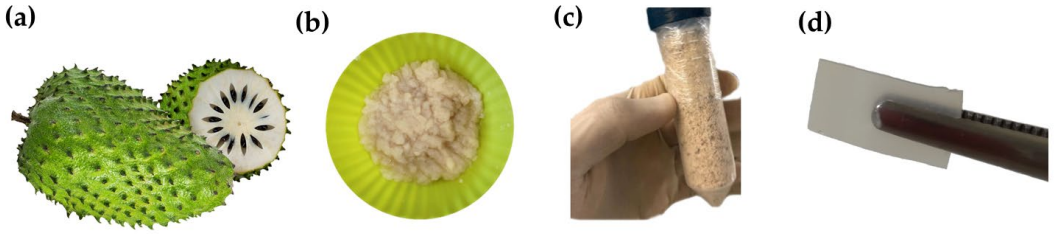

Figure 1. Soursop fruit (*Annona muricata* L.) (**a**); hydrated biopolymer from *A. muricata residues* (Biop_AmRs) (**b**); Biop_AmRs after purification and drying (**c**); and (**d**) Film of Biop_AmRs with glycerol.

In this study, ethanol, an environmentally friendly solvent, was used to purify the Biop_AmRs. Ethanol is a low-cost solvent, with lower toxicity in comparison to fossil solvents. Ethanol is classified as a green solvent due to its availability through the fermentation of renewable sources [29]. In the food industry, the use of toxic organic solvents has been replaced by the use of green solvents. Green solvents are in agreement with environmental, safety, and health characteristics [30]. Thus, the green extraction of the Biop_AmRs adds value to the obtained input.

3.2. Characterization of Biop_AmRs

The Biop_AmRs presents a pH of 5.14 ± 0.06 and a conductivity of 331.23 ± 0.83 μS cm^{-1}. These results are related to the ionizable acid moieties present within the polymer chains. The industrial polysaccharides gum arabic, pectin, and alginate demonstrate analogous behavior due to their composition of sugar acids [31].

According to Cano-Sarmiento et al. [32], zeta potential is an important indicator to evaluate electrical interactions in food systems, which has been used to characterize food waste. The zeta potential value for the Biop_AmRs was −33.50 ± 0.05 mV, indicating that this material has an anionic character, which may be related to the presence of anionic functional groups, such as hydroxyl and carboxyl, on the structure of the sample [33,34]. Very similar negative zeta potentials were obtained in natural biopolymers, such as pectin (−31.30 ± 0.14 mV), xanthan gum (−33.20 ± 0.10 mV) [35], and alginate (−29.94 ± 1.45 mV) [31]. Zeta potential has been used to determine the ionic nature and colloidal properties of polysaccharides, and almost all natural polysaccharides have negative charges [35,36]. Zeta potential is one of the most important parameters indicating the stability of colloidal dispersions. Dispersions with values around ±30 mV have high repulsive force to prevent aggregation or flocculation, indicating the formation of highly stable colloidal dispersions [32,37]. Thus, this result indicates the formation of a stable colloidal system that can be attractive to pharmaceutical, cosmetic, and food applications [38].

Three peaks corresponding to molecular weights (Mw) of 183.14 kDa, 27.52 kDa, and 0.16 KDa were detected in the crude polysaccharide of *A. muricata* residues (Biop_AmRs). The extraction process can affect the molecular mass of polysaccharides, as shown by Lopes Leivas et al. [4] in their work on the extraction and characterization of polysaccharides from the soluble and insoluble fibers of soursop fruit.

Table 1 shows the biopolymer's monosaccharide and uronic acid composition. This result demonstrates that the material consists of a heteropolysaccharide, which is composed of the following five neutral monosaccharides: arabinose (Ara, 10.0 mol %), xylose (Xyl, 10.0 mol %), mannose (Man, 3.0 mol %), galactose (Gal, 6.0 mol %), and glucose (Glc, 42.0 mol %). The results also indicated the presence of uronic acid (UA, 28.0 mol %).

Table 1. Chemical composition of biopolymer from *A. muricata* residues (Biop_AmRs).

Sample	Composition						
	Monosaccharides (Mol %)					U.A. Total (mg g^{-1})	
	Ara	Xyl	Man	Gal	Glc		
Bio_AmRs	10.0	10.0	3.0	6.0	42.0	28.0	505.88

Bio_AmRs: biopolymer from *A. mirucata* fruit residues. Ara: arabinose. Xyl: xylose. Man: mannose. Gal: galactose. Glc: glucose. U.A.: uronic acid.

The predominant monomers identified in this simple were arabinose, xylose, and glucose. According to Berumen-Varela et al. [3], the white pulp of soursop predominantly consists of water and carbohydrates. Several studies with fruit pulps have shown a varied monosaccharide profile [28,39]. This carbohydrate profile may be related to the polysaccharides in the fruit pulp, such as the pectins. Pectins are abundant in the waste of fruits and can be separated from most of the other components through precipitation in ethanol [40,41]. A complex study conducted by Lopes Leivas and collaborators [4] of fractions obtained from the aqueous and alkaline extracts of pulp from soursop fruits (*A. muricata*) detected the presence of arabinose, xylose, galactose, glucose, rhamnose, fucose, and uronic acids. The polysaccharides in the obtained fractions were characterized as homogalacturonan, type II arabinogalactan, pectic arabinan, xylan-xyloglucan, and acid xylan [4].

Fruit wastes contain variable amounts of proteins [42]. The protein content of the Biop_AmRs sample in this study was 19.77 ± 0.66%. Agu and Okolie [43] determined the proximal composition of the *Annona muricata* fruit and recorded 10.9% of crude protein.

The higher concentration of proteins found in the Biop_AmRs may be attributed to the extraction technique and concentration with drying.

Figure 2 presents the FTIR spectrum of the Biop_AmRs. The FTIR spectrum displayed bands ranging from 1031 to 3350 cm^{-1}, which is typical of scaffold vibrations for polysaccharides. The absorption peak at 3350 cm^{-1} indicates an O–H group stretching vibration. The bands at 2925 cm^{-1} and 2854 cm^{-1} are related to C–H stretching vibrations [44]. Absorption was observed at the peak of 1743 cm^{-1} derived from the stretching vibration of the C=O carbonyl groups [45]. The absorption peak around 1740 cm^{-1}, corresponds to the presence of uronic acid in the polysaccharide structure [46]. The band at 1636 cm^{-1} is characteristic of the structure of a protein [47]. The 1031 cm^{-1} peak is associated with a region that is considered the fingerprint of all polysaccharides [48]. The presence of absorption bands in the range of 1400 cm^{-1} to 987 cm^{-1} seen in the sample indicates the presence of pectin polysaccharide rich in uronic acids and xylans [49].

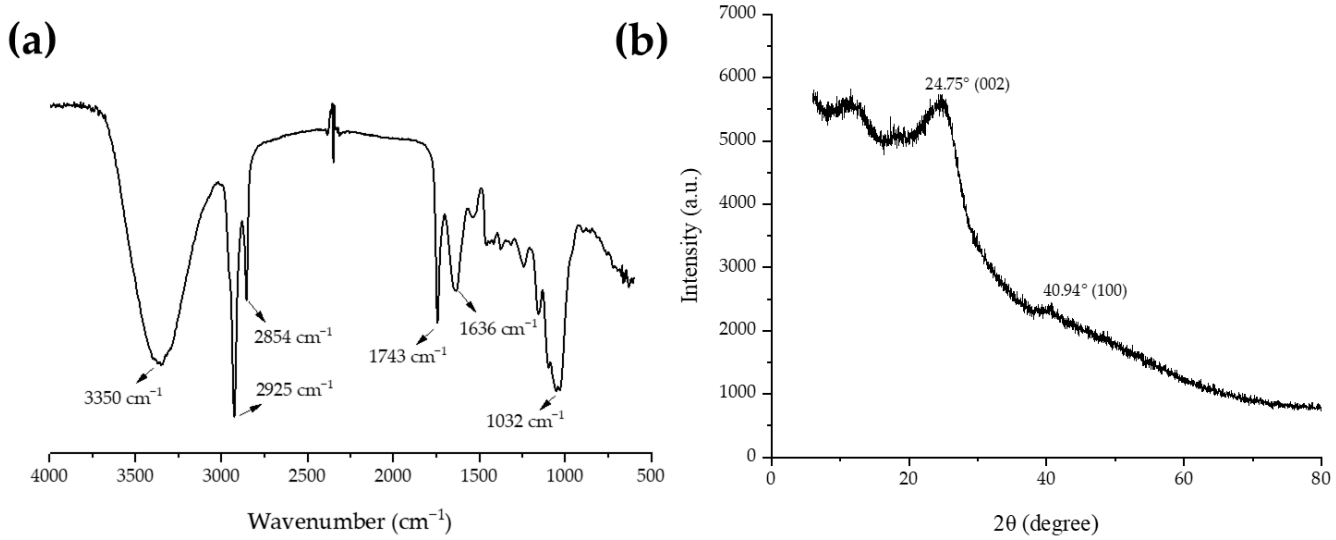

Figure 2. (**a**) Fourier transform infrared spectrum (FTIR) of Biop_AmRs; (**b**) X-ray diffractogram of Biop_AmRs.

The X-ray diffraction patterns of the Biop_AmRs are presented in Figure 2. The Biop_AmRs diffractogram exhibited a characteristic amorphous halo and peaks at 2θ = 11.5°, 24.75°, and 40.94°. According to the pectin analysis performed by Wahid et al. [50], the peak around 24.6° and 43.7° corresponds to the 002 and 100 plane of carbon, respectively. This result characterizes this polysaccharide as semicrystalline [51]. It is possible to observe a semicrystalline profile similar to that of the pectin sample, which reinforces the results obtained using FTIR and chemical analyses [52].

Thermoanalytical analyses are widely used to test raw materials, demonstrate the stability and compatibility of ingredients, and obtain new formulations. In this study, the thermal stability and the decomposition of the Biop_AmRs were examined using TGA, DTG, and DSC, and the results are shown in Figure 3. It is noted that there is a three-step degradation pattern for the sample. The first mass loss stage starts around 50 °C and corresponds to about a 10% mass loss of water in the sample. This loss may be related to hygroscopic moisture and the condensation of hydroxyl groups on the surface of the sample [53,54]. The second mass loss event starts at about 250 °C to 300 °C and corresponds to the main mass loss in a total of 50% of the sample; this stage involves the alteration of functional groups and depolymerization of polymeric structures [55]. The third stage, between 450 °C and 500 °C, corresponds to the oxidation range. The DTG curve (Figure 3a) shows that the Biop_AmRs has a temperature of maximum weight loss rate (Tmwl) of approximately 493 °C. The temperature of maximum weight loss rate (Tmwl) determines the thermal stability of a material. A higher Tmwl indicates greater thermal stability [56]. A

similar thermal profile has been observed for other polysaccharides, including pectin [52,57]. The Biop_AmRs demonstrated favorable thermal stability and potential for use in the food and pharmaceutical industries.

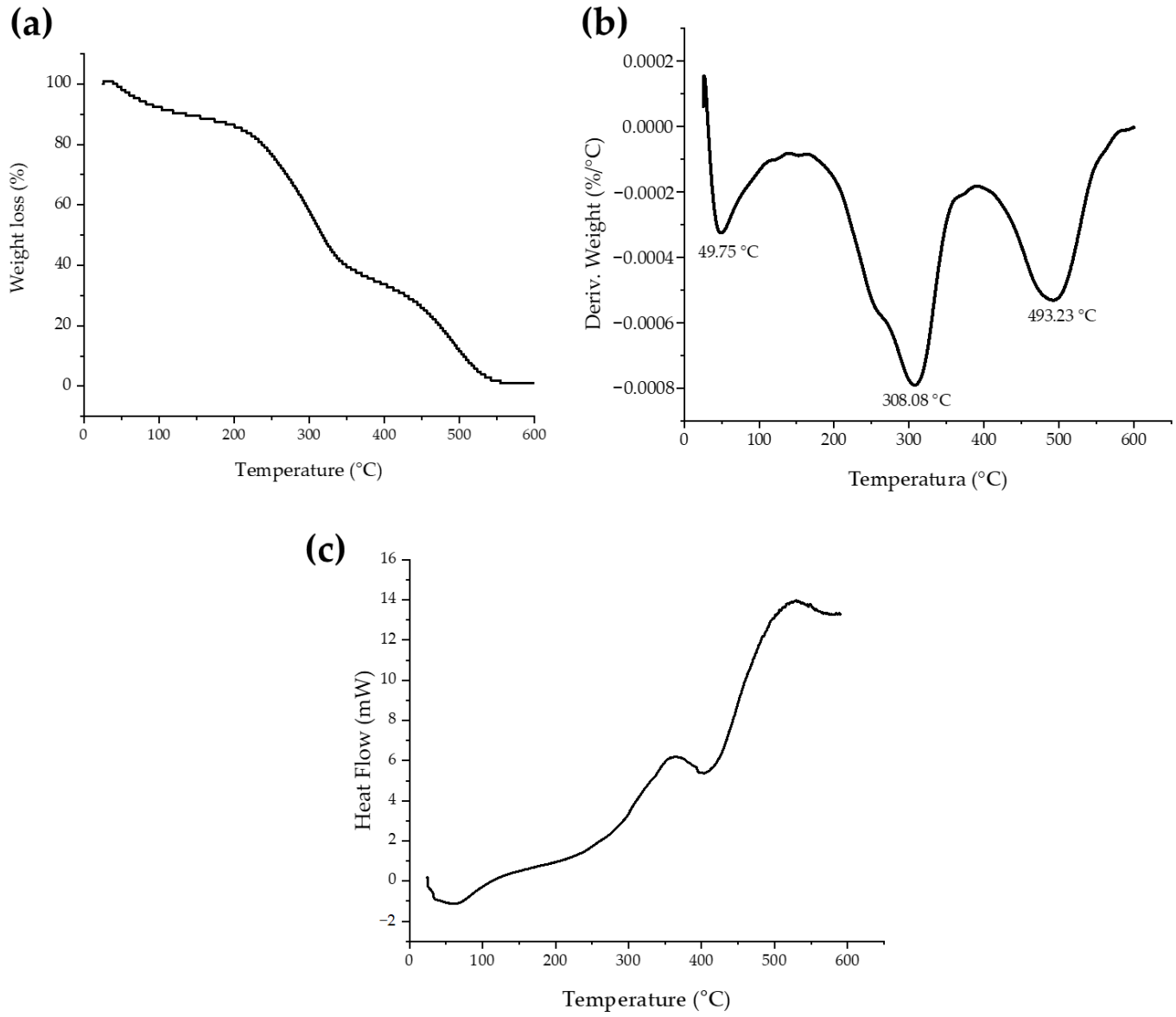

Figure 3. TGA (**a**), DTG (**b**), and DSC (**c**) curves for Biop_AmRs at an inert air and heating rate of 10 °C min^{-1}.

In Figure 4, it is possible to observe the electron micrograph of the Biop_AmRs powder. The Biop_AmRs micrographs showed a spongy, rough, and irregular material. According to Joulak et al. [58], the morphology of polysaccharides can influence their functional, sensory, and physical properties. It is important to note that fibrous aggregates of non-uniform size and distribution affect the intrinsic viscosity and molecular weight of the polymer. Furthermore, as the size of the surface area of a particle increases, consequently, its hydration capacity increases [59]. Polymers that hydrate and swell are important pharmaceutical excipients in controlled drug release matrices [60].

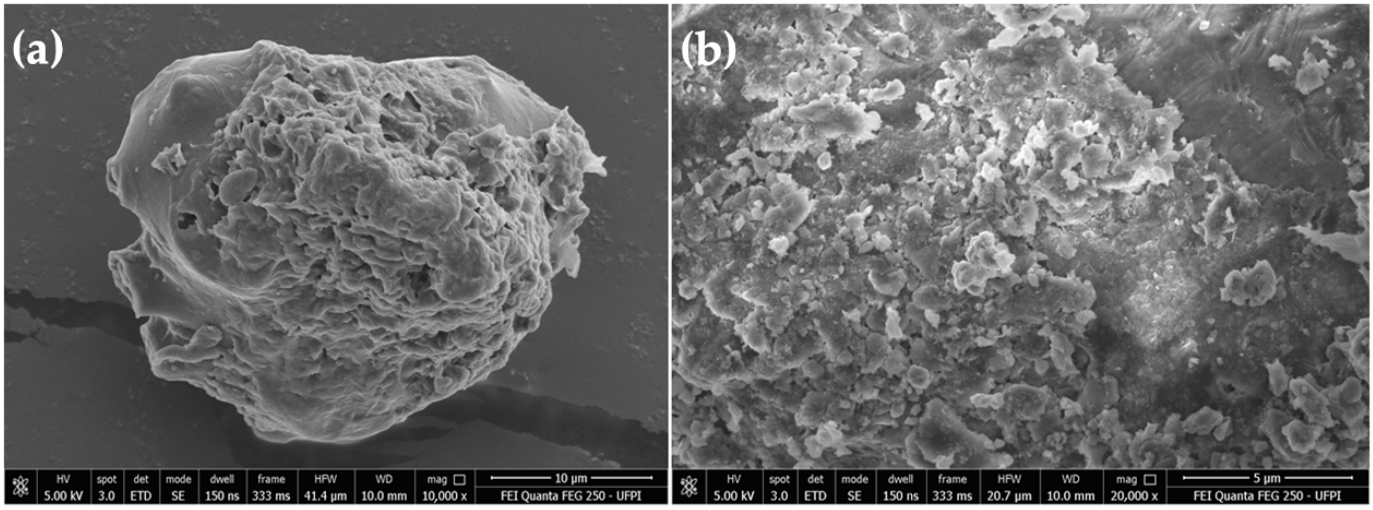

Figure 4. Biop_AmRs micrographs at magnifications of (**a**) 10,000× and (**b**) 20,000×.

Films with the Biop_AmRs were obtained using the casting method (Figure 1d). These films presented homogeneity, transparency, and flexibility. Casting is the most common technique for obtaining pectin films (2–3 wt%) containing mainly glycerol as a plasticizer. Films made from biopolymers have several advantages compared to synthetic polymers, including biodegradability, non-toxicity, renewability, waste reduction, environmental friendliness, and others [16]. Film-forming polymers present versatile industrial applications. These polymeric films may be applicable in tablet coatings, transdermal patches, wound dressings, and different drug deliveries [60,61]. In the food industry, films or coatings, including carriers of active compounds, have been widely used [62].

The functional properties of polysaccharides are influenced by the structure, molecular weight, chemical composition, and type of glycosidic bonds [63]. Table 2 shows the results of the technological properties of the Biop_AmRs.

Table 2. Technological properties of the biopolymer from *A. muricata residues* (Biop_AmRs).

Functional Properties	Results (%)
Water holding capacity	47.50 ± 0.33
Emulsifying capacity	97.33 ± 4.62
Emulsifying stabilization	40.00 ± 0.00
Foaming ability	Absence

The Biop_AmRs has a water holding capacity (WHC) of 47.50%. This high water uptake is proportional to the unfolding of the polysaccharide chains [64]. WHC is one of the most important functional properties and represents the amount of water retained by 1 g of dry sample [65,66]. This property is also related to the texture of the polymer, as it depends on the interaction of water with it [67]. This is an attractive property for the food industry, as the polymer can be applied as a stabilizer and texture modifier [68]. Interesting results of the emulsifying properties of the Biop_AmRs are shown in Table 1. An interesting property of natural polysaccharides is their emulsifying capacity (EC). The EC of the biopolymer was 97.33%, showing that the sample has a high emulsifying activity. Jeddou et al. [69] obtained values greater than 90% of the emulsifying capacity of the potato polysaccharide. The emulsifying stabilization (ES) of the biopolymer was 40%. Spinel and Oroian [66] presented similar ES results for citrus pectin (40.22%) and grape pomace pectin (40.02%). Emulsions are formulations that are considered thermodynamically unstable and require additives to prevent the loss of system stability. The ability to form and stabilize emulsions is a major attraction in the use of new ingredients with industrial potential, including polysaccharides and proteins, which are important components involved in

emulsifying properties [66,70]. Therefore, emulsifiers increase the viscosity and improve the stability and texture of food and pharmaceutical products [53,71]. Gheribi et al. [72] define foam as gas bubbles dispersed in an aqueous phase. This property imparts flexibility to the biopolymer and is related to the composition of the polysaccharide, which in this case, did not exhibit foam formation [21]. These results indicate that the Biop_AmRs has a promising potential as emulsifiers and stabilizers in food, cosmetic, and pharmaceutical formulations but are not able to form foam.

In this study, the texturometric parameters (firmness, consistency, cohesiveness, and viscosity index) of the Biop_AmRs were compared with two biopolymers that are popularly used in the food, cosmetic, and pharmaceutical industries. The results of the texturometric analysis can be seen in Figure 5.

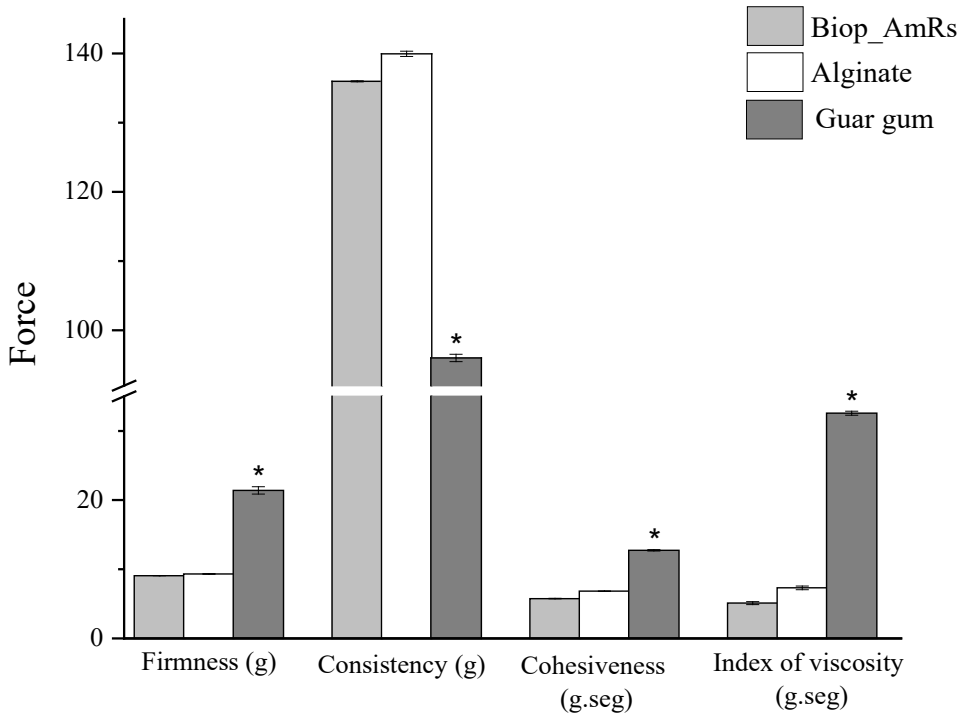

Figure 5. Texturometric parameters of the *A. muricata* residues (Biop_AmRs) at 1 wt% compared to alginate and guar gum. * $p < 0.05$.

It was possible to observe that the parameters of firmness, consistency, cohesiveness, and viscosity index of the Biop_AmRs were comparable to alginate, an anionic biopolymer derived from algae with excellent physicochemical properties [73]. The similar firmness and consistency values for the biopolymer and alginate samples may represent similar viscosity and spreadability characteristics of cosmetic or pharmaceutical products [74,75]. Texture testing can help guide the development of new products with more attractive mechanical properties [76,77].

The results of the mucoadhesiveness are shown in Figure 6. The Biop_AmRs powder presented an adhesion force (Fmax) of 0.093 ± 0.005 N and work of adhesion (Wad) of 0.030 ± 0.005 N.s. Mucoadhesion is a complex process that involves intimate contact between two surfaces, one of which must be a mucosal tissue or membrane and the other a mucoadhesive material [78,79]. This process occurs in two stages, the first related to the first contact between the mucoadhesive material and the mucosa and the second, the consolidation phase, involving secondary physical and chemical interactions such as hydrogen bonds, van der Waals forces, and electrical attractions [80]. In general, polymers that have many hydrophilic groups have a higher mucoadhesive potential; this ability is strongly impacted by a variety of variables, including chain flexibility, molar mass, molecular charge, crosslinking density, ionic strength, and moisture level [81].

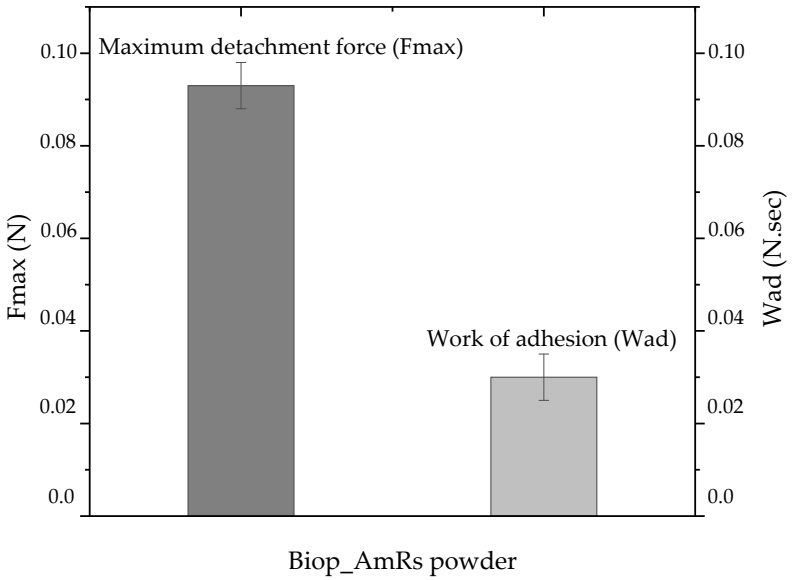

Figure 6. Mucoadhesive properties of the Biop_AmRs sample.

The Biop_AmRs showed an Fmax of 0.093 ± 0.005 N (93.33 mN), which was higher than that observed by Freitas et al. [82] in natural and modified chichá gum (74.78 ± 1.09 mN and 81.85 ± 0.17 mN, respectively). The mucoadhesive properties of the Biop_AmRs are important for their application in the biomedical and pharmaceutical fields. It allows the development of mucoadhesive drug delivery devices, including films and tablets.

The results obtained for the cytocompatibility analysis of the Biop_AmRs are in Figure 7a. A survival rate above 95% was observed for all concentrations tested, indicating that the Biop_AmRs did not present cytotoxicity for the concentrations tested in the used strains. Cytotoxicity is described as the toxic effects of materials on biological tissues. In this context, cell viability assays are important to assess cell damage from potentially toxic substances [83]. According to ISO (ISO, 2009), a compound with a cell viability inhibition percentage above 30% is cytotoxic. Moreover, a compound with a cell viability inhibition percentage above 70% is considered a cytocompatible material. New raw materials for applications in healthcare devices should not be toxic or present adverse responses in the site and surrounding the applications. Due to this, before the preclinical or clinical evaluation stages of new medical biomaterials, the cytocompatibility of the inputs must be known [84].

The Biop_AmRs did not form a hemolytic halo in the blood agar, which indicates that this biomaterial is hemocompatible (Figure 7b). Polymeric materials with promising properties for use in medical devices or drug delivery systems are evaluated for hemocompatibility. Materials that may cause blood-related adverse events have limited biomedical applications; therefore, the hemolysis test is essential for assessing the hemocompatibility of materials intended to be applied in biological systems [85,86]. Moreover, it may come into contact with blood since damage to erythrocytes resulting in the release of hemoglobin is considered the first evidence of cytotoxicity in human cells [87]. This result corroborates the results obtained in the cytotoxicity analysis.

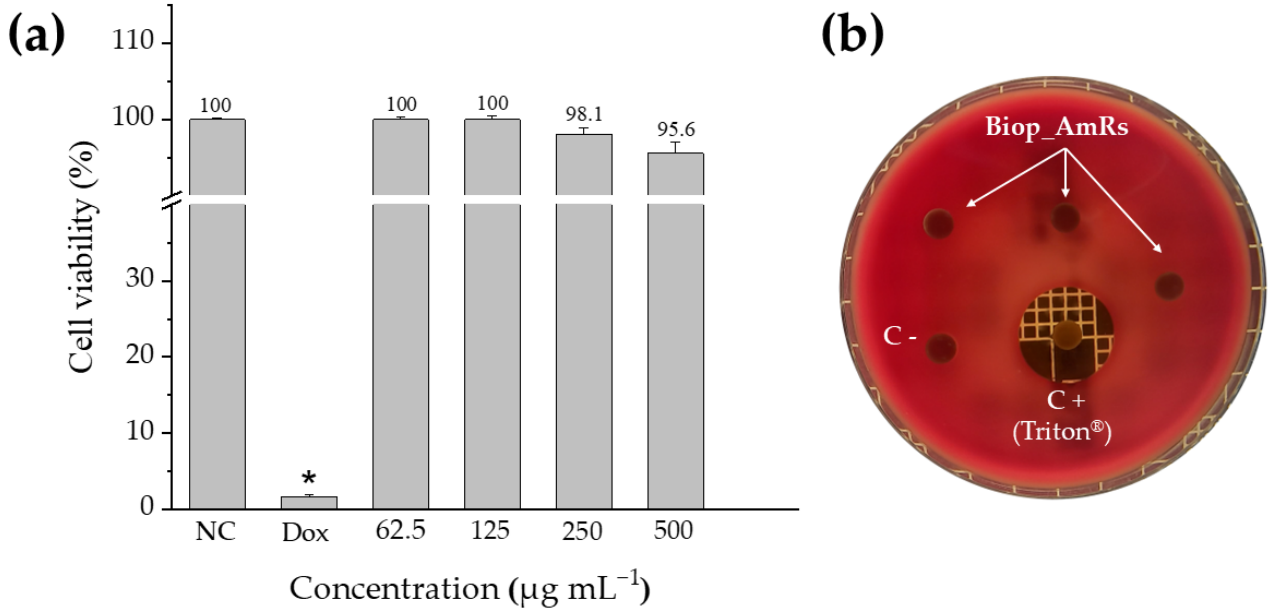

Figure 7. (**a**) Cell viability percentage of the Biop_AmRs evaluated using the MTT test after 72 h of exposure on the L929 cell line. (Triplicate assays; mean ± SEM), NC: negative control. Doxorrubicin (Dox) was used as a positive control. (**b**) Blood agar plate with Biop_AmRs sample and negative and positive controls (Triton). * $p < 0.05$ vs. NC of Dox using Dunnet's *t*-test.

4. Conclusions

In this study, it was possible to observe promising properties of the biopolymer from *A. muricata* fruit residues (Biop_AmRs). The Biop_AmRs is an anionic heteropolysaccharide with semicrystalline characteristics, an excellent water holding capacity, and good emulsifying and mucoadhesive properties. The biopolymer also showed cytocompatibility on the L929 cell line, as well as hemocompatibility. These findings identify the Biop_AmRs as a potential environmentally friendly raw material for use in the food, pharmaceutical, biomedical, and cosmetic industries.

Author Contributions: Conceptualization and methodology: I.F.S.R., S.C.D., T.B.C.L., R.d.A. and F.T.d.S.S.J.; validation: I.F.S.R., S.C.D. and S.J.C.G.; formal analysis: I.F.S.R., S.C.D., M.A., Ó.R. and M.P.C.; writing—original draft preparation: I.F.S.R., T.B.C.L. and S.C.D.; supervision: A.B.R., M.P.C., E.C.S.-F. and J.A.O.; writing—review and editing: M.P.C., E.C.S.-F., M.S.R. and A.B.R.; project administration: M.P.C., M.S.R. and A.B.R.; funding acquisition: C.P., E.C.S.-F., M.S.R., M.P.C., J.A.O. and S.J.C.G. All authors have read and agreed to the published version of the manuscript.

Funding: This study was supported by the Conselho Nacional de Desenvolvimento Científico e Tecnológico—Brazil (CNPq) and the Coordenação de Aperfeiçoamento de Pessoal de Nível Superior—Brazil (CAPES) in the form of scholarship (# 88882.446231/2019-01).

Institutional Review Board Statement: Not applicable.

Data Availability Statement: All data obtained in this study are included in this article.

Acknowledgments: The authors are grateful to LIMAV/UFPI and UFC for structural support.

Conflicts of Interest: The authors declare no conflicts of interest.

References

1. Do, Y.V.; Le, Q.N.T.; Nghia, N.H.; Vu, N.D.; Tran, N.T.Y.; Bay, N.T.; Tran, T.T.; Bach, L.G.; Dao, T.P. Assessment of the changes in product characteristics, total ascorbic acid, total flavonoid content, total polyphenol content and antioxidant activity of dried soursop fruit tea (*Annona muricata* L.) during product storage. *Food Sci. Nutr.* **2024**, *12*, 2679–2691. [CrossRef] [PubMed]
2. Coria-Téllez, A.V.; Montalvo-Gónzalez, E.; Yahia, E.M.; Obledo-Vázquez, E.N. *Annona muricata*: A comprehensive review on its traditional medicinal uses, phytochemicals, pharmacological activities, mechanisms of action and toxicity. *Arab. J. Chem.* **2018**, *11*, 662–691. [CrossRef]
3. Berumen-Varela, G.; Hernández-Oñate, M.A.; Tiznado-Hernández, M.E. Utilization of biotechnological tools in soursop (*Annona muricata* L.). *Sci. Horticul.* **2019**, *245*, 269–273. [CrossRef]
4. Lopes Leivas, C.; Moro Cantu-Jungles, T.; Barbosa da Luz, B.; Fernanda de Paula Werner, M.; Iacomini, M.; MC Cordeiro, L. Investigation of the chemical structure and analgesic and anti-inflammatory properties of polysaccharides that constitute the dietary fibers of soursop (*Annona muricata*) fruit. *Food Res. Int.* **2023**, *166*, 112588. [CrossRef]
5. Santos, I.L.; Rodrigues, A.M.D.C.; Amante, E.R.; Silva, L.H.M.D. Soursop (*Annona muricata*) Properties and Perspectives for Integral Valorization. *Foods* **2023**, *12*, 1448. [CrossRef] [PubMed]
6. Slorach, P.C.; Jeswani, H.K.; Cuéllar-Franca, R.; Azapagic, A. Environmental sustainability of anaerobic digestion of household food waste. *J. Environ. Manag.* **2019**, *236*, 798–814. [CrossRef] [PubMed]
7. Nor, S.M.; Ding, P. Trends and advances in edible biopolymer coating for tropical fruit: A review. *Food Res. Int.* **2020**, *134*, 109208. [CrossRef]
8. Caldeira, C.; Vlysidis, A.; Fiore, G.; De Laurentiis, V.; Vignali, G.; Sala, S. Sustainability of food waste biorefinery: A review on valorisation pathways, techno-economic constraints, and environmental assessment. *Bioresour. Technol.* **2020**, *312*, 123575. [CrossRef]
9. Meng, X.; Liang, H.; Luo, L. Antitumor polysaccharides from mushrooms: A review on the structural characteristics, antitumor mechanisms and immunomodulating activities. *Carbohydr. Res.* **2016**, *424*, 30–41. [CrossRef]
10. Xie, M.-Y. Sulfated modification, characterization and antioxidant activities of polysaccharide from *Cyclocarya paliurus*. *Food Hydrocoll.* **2016**, *53*, 7–15. [CrossRef]
11. Plucinski, A.; Lyu, Z.; Schmidt, B.V.K.J. Polysaccharide nanoparticles: From fabrication to applications. *J. Mater. Chem. B* **2021**, *9*, 7030–7062. [CrossRef] [PubMed]
12. Funami, T. In vivo and rheological approaches for characterizing food oral processing and usefulness of polysaccharides as texture modifiers—A review. *Food Hydrocoll.* **2017**, *68*, 2–14. [CrossRef]
13. Yu, Y.; Shen, M.; Song, Q.; Xie, J. Biological activities and pharmaceutical applications of polysaccharide from natural resources: A review. *Carbohydr. Polym.* **2018**, *183*, 91–101. [CrossRef]
14. Liu, J.; Wang, X.; Yong, H.; Kan, J.; Jin, C.C. Recent advances in flavonoid-grafted polysaccharides: Synthesis, structural characterization, bioactivities and potential applications. *Int. J. Biol. Macrom.* **2018**, *116*, 1011–1025. [CrossRef]
15. Isopencu, G.O.; Covaliu-Mierlă, C.-I.; Deleanu, I.-M. From Plants to Wound Dressing and Transdermal Delivery of Bioactive Compounds. *Plants* **2023**, *12*, 2661. [CrossRef]
16. Mellinas, C.; Ramos, M.; Jiménez, A.; Garrigós, M.C. Recent Trends in the Use of Pectin from Agro-Waste Residues as a Natural-Based Biopolymer for Food Packaging Applications. *Materials* **2020**, *13*, 673. [CrossRef] [PubMed]
17. George, A.; Sanjay, M.R.; Sriusk, R.; Parameswaranpillai, J.; Siengchin, S. A comprehensive review on chemical properties and applications of biopolymers and their composites. *Int. J. Biol. Macrom.* **2020**, *154*, 329–338. [CrossRef] [PubMed]
18. Muñoz, L.A.; Aguilera, J.M.; Rodriguez-Turienzo, L.; Cobos, A.; Diaz, O. Characterization and microstructure of films made from mucilage of Salvia hispanica and whey protein concentrate. *J. Food Eng.* **2012**, *111*, 511–518. [CrossRef]
19. Coelho, E.; Rocha, M.A.M.; Moreira, A.S.; Domingues, M.R.M.; Coimbra, M.A. Revisiting the structural features of arabinoxylans from brewers' spent grain. *Carbohydr. Polym.* **2016**, *139*, 167–176. [CrossRef]
20. Mæhre, H.K.; Dalheim, L.; Edvinsen, G.K.; Elvevoll, E.O.; Jensen, I.J. Protein Determination-Method Matters. *Foods* **2018**, *7*, 5. [CrossRef]
21. Alpizar-Reyes, E.; Carrillo-Navas, H.; Gallardo-Rivera, R.; Varela-Guerrero, V.; Alvarez-Ramirez, J.; Pérez-Alonso, C. Functional properties and physicochemical characteristics of tamarind (*Tamarindus indica* L.) seed mucilage powder as a novel hydrocolloid. *J. Food Eng.* **2017**, *209*, 68–75. [CrossRef]
22. Davidović, S.; Miljković, M.; Tomić, M.; Gordić, M.; Nešić, A.; Dimitrijević, S. Response surface methodology for optimisation of edible coatings based on dextran from Leuconostoc mesenteroides T3. *Carbohydr. Polym.* **2018**, *184*, 207–213. [CrossRef] [PubMed]
23. Ramos, I.F.S.; Magalhães, L.M.; do O Pessoa, C.; Ferreira, P.M.P.; dos Santos Rizzo, M.; Osajima, J.A.; Silva-filho, E.C.; Costa, M.P. New properties of chia seed mucilage (*Salvia hispanica* L.) and potential application in cosmetic and pharmaceutical products. *Ind. Crops Prod.* **2021**, *171*, 113981. [CrossRef]
24. Thirawong, N.; Nunthanid, J.; Puttipipatkhachorn, S.; Sriamornsak, P. Mucoadhesive properties of various pectins on gastrointestinal mucosa: An in vitro evaluation using texture analyzer. *Eur. J. Pharm. Biopharm.* **2007**, *67*, 132–140. [CrossRef] [PubMed]
25. Soe, M.T.; Chitropas, P.; Pongjanyakul, T.; Limpongsa, E.; Jaipakdee, N. Thai glutinous rice starch modified by ball milling and its application as a mucoadhesive polymer. *Carbohydr. Polym.* **2020**, *232*, 115812. [CrossRef]

26. *ISO 10993-5: 2009*; Tests for In Vitro Cytotoxicity. In Biological Evaluation of Medical Devices. International Organization for Standardization: Geneva, Switzerland, 2009; Volume 34.
27. Kalegari, M.; Miguel, M.D.; Dias, J.D.F.G.; Lordello, A.L.L.; Lima, C.P.D.; Miyazaki, C.M.S.; Zanin, S.M.W.; Verdam, M.C.S.; Miguel, O.G. Phytochemical constituents and preliminary toxicity evaluation of leaves from *Rourea induta* Planch. (*Connaraceae*). *Braz. J. Pharm. Sci.* **2011**, *47*, 635–642. [CrossRef]
28. Ren, Y.; Zhu, Z.; Sun, H.; Chen, L. Structural characterization and inhibition on α-glucosidase activity of acidic polysaccharide from Annona squamosa. *Carbohydr. Polym.* **2017**, *174*, 1–12. [CrossRef]
29. Tekin, K.; Hao, N.; Karagoz, S.; Ragauskas, A.J. Ethanol: A Promising Green Solvent for the Deconstruction of Lignocellulose. *ChemSusChem* **2018**, *11*, 3559–3575. [CrossRef]
30. Kamal, H.; Ali, A.; Le, C.F. Green solvent processing: Effect of type of solvent on extraction and quality of protein from dairy and non-dairy expired milk products. *Food Chem.* **2023**, *400*, 133988. [CrossRef]
31. Barbosa, J.A.; Abdelsadig, M.S.; Conway, B.R.; Merchant, H.A. Using zeta potential to study the ionisation behaviour of polymers employed in modified-release dosage forms and estimating their pKa. *Int. J. Pharm. X* **2019**, *1*, 100024. [CrossRef]
32. Cano-Sarmiento, C.; Téllez-Medina, D.I.; Viveros-Contreras, R.; Cornejo-Mazón, M.; Figueroa-Hernández, C.Y.; García-Armenta, E.; Alamilla-Beltrán, L.; García, H.S.; Gutiérrez-López, F. Zeta Potential of Food Matrices. *Food Eng. Rev.* **2018**, *10*, 113–138. [CrossRef]
33. Pathak, P.O.; Nagarsenker, M.S.; Barhate, C.R.; Padhye, S.G.; Dhawan, V.V.; Bhattacharyya, D.; Viswanathan, C.L.; Steiniger, F.; Fahr, A. Cholesterol anchored arabinogalactan for asialoglycoprotein receptor targeting: Synthesis, characterization, and proof of concept of hepatospecific delivery. *Carbohydr. Res.* **2015**, *408*, 33–43. [CrossRef]
34. Bratuša, A.; Elschner, T.; Heinze, T.; Fröhlich, E.; Hribernik, S.; Božič, M.; Žagar, E.; Kleinschek, K.S.; Thonhofer, M.; Kargl, R. Functional dextran amino acid ester particles derived from N-protected S-trityl-L-cysteine. *Colloids Surf. B Biointerfaces* **2019**, *181*, 561–566. [CrossRef]
35. Ren, H.; Li, Z.; Gao, R.; Zhao, T.; Luo, D.; Yu, Z.; Zhang, S.; Qi, C.; Wang, Y.; Qiao, H.; et al. Structural Characteristics of *Rehmannia glutinosa* Polysaccharides Treated Using Different Decolorization Processes and Their Antioxidant Effects in Intestinal Epithelial Cells. *Foods* **2022**, *11*, 3449. [CrossRef]
36. Andrew, M.; Jayaraman, G. Molecular Characterization and Biocompatibility of Exopolysaccharide Produced by Moderately Halophilic Bacterium *Virgibacillus dokdonensis* from the Saltern of Kumta Coast. *Polymers* **2022**, *14*, 3986. [CrossRef] [PubMed]
37. Lucena, M.d.A.; Ramos, I.F.d.S.; Geronço, M.S.; de Araújo, R.; da Silva Filho, F.L.; da Silva, L.M.L.R.; de Sousa, R.W.R.; Ferreira, P.M.P.; Osajima, J.A.; Silva-Filho, E.C.; et al. Biopolymer from Water Kefir as a Potential Clean-Label Ingredient for Health Applications: Evaluation of New Properties. *Molecules* **2022**, *27*, 3895. [CrossRef] [PubMed]
38. Sibaja-Hernández, R.; Román-Guerrero, A.; Sepúlveda-Jiménez, G.; Rodríguez- Monroy, M. Physicochemical, shear flow behaviour and emulsifying properties of *Acacia cochliacantha* and *Acacia farnesiana* gums. *Ind. Crops Prod.* **2015**, *67*, 161–168. [CrossRef]
39. Colodel, C.; Bagatin, R.M.D.G.; Tavares, T.M.; Petkowicz, C.L.O. Cell wall polysaccharides from pulp and peel of cubiu: A pectin-rich fruit. *Carbohydr. Polym.* **2017**, *174*, 226–234. [CrossRef]
40. Lara-Espinoza, C.; Carvajal-Millán, E.; Balandrán-Quintana, R.; López-Franco, Y.; Rascón-Chu, A. Pectin and Pectin-Based Composite Materials: Beyond Food Texture. *Molecules* **2018**, *23*, 942. [CrossRef]
41. Pascoalino, L.A.; Reis, F.S.; Prieto, M.A.; Barreira, J.C.M.; Ferreira, I.C.F.R.; Barros, L. Valorization of Bio-Residues from the Processing of Main Portuguese Fruit Crops: From Discarded Waste to Health Promoting Compounds. *Molecules* **2021**, *26*, 2624. [CrossRef]
42. Sha, S.P.; Modak, D.; Sarkar, S.; Roy, S.K.; Sah, S.P.; Ghatani, K.; Bhattacharjee, S. Fruit waste: A current perspective for the sustainable production of pharmacological, nutraceutical, and bioactive resources. *Front. Microbiol.* **2023**, *14*, 1260071. [CrossRef] [PubMed]
43. Agu, K.C.; Okolie, P.N. Proximate composition, phytochemical analysis, and in vitro antioxidant potentials of extracts of *Annona muricata* (Soursop). *Food Sci. Nutr.* **2017**, *5*, 1029–1036. [CrossRef] [PubMed]
44. Sun, M.; Li, Y.; Wang, T.; Sun, Y.; Xu, X.; Zhang, Z. Isolation, fine structure and morphology studies of galactomannan from endosperm of *Gleditsia japonica* var. delavayi. *Carbohydr. Polym.* **2018**, *184*, 127–134. [CrossRef]
45. Silva, S.H.; Neves, I.C.O.; Oliveira, N.L.; De Oliveira, A.C.F.; Lago, A.M.T.; De Oliveira Giarola, T.M.; De Resende, J.V. Extraction processes and characterization of the mucilage obtained from green fruits of *Pereskia aculeata* Miller. *Ind. Crops Prod.* **2019**, *140*, 111716. [CrossRef]
46. Tu, W.; Zhu, J.; Bi, S.; Chen, D.; Song, L.; Wang, L.; Zi, J.; Yu, R. Isolation, characterization and bioactivities of a new polysaccharide from Annona squamosa and its sulfated derivative. *Carbohydr. Polym.* **2016**, *152*, 287–296. [CrossRef] [PubMed]
47. Sadat, A.; Joye, I.J. Peak Fitting Applied to Fourier Transform Infrared and Raman Spectroscopic Analysis of Proteins. *Appl. Sci.* **2020**, *10*, 5918. [CrossRef]
48. Shi, K.; An, W.; Meng, Q.; Gu, Y.; Liu, S. Partial characterization and lyoprotective activity of exopolysaccharide from *Oenococcus oeni* 28A-1. *Process Biochem.* **2021**, *101*, 128–136. [CrossRef]
49. Coimbra, M.A.; Barros, A.; Rutledge, D.N.; Delgadillo, I. FTIR spectroscopy as a tool for the analysis of olive pulp cell-wall polysaccharide extracts. *Carbohydr. Polym.* **1999**, *317*, 145–154. [CrossRef]

50. Wahid, M.; Parte, G.; Fernandes, R.; Kothari, D.; Ogale, S. Natural-gel derived, N-doped, ordered and interconnected 1D nanocarbon threads as efficient supercapacitor electrode materials. *RSC Adv.* **2015**, *5*, 51382–51391. [CrossRef]
51. Fonseca, L.R.; Santos, T.P.; Czaikoski, A.; Cunha, R.L. Modulating properties of polysaccharides nanocomplexes from enzymatic hydrolysis of chitosan. *Food Res. Int.* **2020**, *137*, 109642. [CrossRef]
52. Monfregola, L.; Bugatti, V.; Amodeo, P.; De Luca, S.; Vittoria, V. Physical and water sorption properties of chemically modified pectin with an environmentally friendly process. *Biomacromolecules* **2011**, *12*, 2311–2318. [CrossRef] [PubMed]
53. Wang, L.; Zhang, B.; Xiao, J.; Huang, Q.; Li, C.; Fu, X. Physicochemical, functional, and biological properties of water-soluble polysaccharides from *Rosa roxburghii* Tratt fruit. *Food Chem.* **2018**, *249*, 127–135. [CrossRef]
54. Faucard, P.; Grimaud, F.; Lourdin, D.; Maigret, J.E.; Moulis, C.; Remaud-Siméon, M.; Putaux, J.; Potocki-Véronèse, G.; Rolland-Sabaté, A. Macromolecular structure and film properties of enzymatically-engineered high molar mass dextrans. *Carbohydr. Polym.* **2018**, *181*, 337–344. [CrossRef]
55. Feng, X.; Wang, P.; Lu, Y.; Zhang, Z.; Yao, C.; Tian, G.; Liu, Q. A Novel Polysaccharide from *Heimioporus retisporus* Displays Hypoglycemic Activity in a Diabetic Mouse Model. *Front. Nutr.* **2022**, *9*, 964948. [CrossRef] [PubMed]
56. Boubkr, L.; Bhakta, A.K.; Snoussi, Y.; Moreira Da Silva, C.; Michely, L.; Jouini, M.; Ammar, S.; Chehimi, M.M. Highly Active Ag-Cu Nanocrystal Catalyst-Coated Brewer's Spent Grain Biochar for the Mineralization of Methyl Orange and Methylene Blue Dye Mixture. *Catalysts* **2022**, *12*, 1475. [CrossRef]
57. Wang, Q.; Liu, S.; Xu, L.; Du, B.; Song, L. Purification, Characterization and Bioactivities of Polysaccharides Extracted from Safflower (*Carthamus tinctorius* L.). *Molecules* **2023**, *28*, 596. [CrossRef]
58. Joulak, I.; Azabou, S.; Finore, I.; Poli, A.; Nicolaus, B.; Donato, P.D.I.; Bkhairia, I.; Dumas, E.; Gharsallaoui, A.; Immirzi, B.; et al. Structural characterization and functional properties of novel exopolysaccharide from the extremely halotolerant Halomonas elongata S6. *Int. J. Biol. Macromol.* **2020**, *164*, 95–104. [CrossRef]
59. Jamir, K.; Badithi, N.; Venumadhav, K.; Seshagirirao, K. Characterization and comparative studies of galactomannans from *Bauhinia vahlii*, *Delonix elata*, and *Peltophorum pterocarpum*. *Int. J. Biol. Macromol.* **2019**, *134*, 498–506. [CrossRef]
60. Choudhury, A.; Sarma, S.; Sarkar, S.; Kumari, M.; Dey, B.K. Polysaccharides Obtained from Vegetables: An effective source of alternative excipient. *J. Pharmacopunct.* **2022**, *25*, 317–325. [CrossRef]
61. Maver, T.; Mohan, T.; Gradišnik, L.; Finšgar, M.; Stana Kleinschek, K.; Maver, U. Polysaccharide Thin Solid Films for Analgesic Drug Delivery and Growth of Human Skin Cells. *Front. Chem.* **2019**, *7*, 217. [CrossRef]
62. Hashemi, S.M.B.; Kaveh, S.; Abedi, E.; Phimolsiripol, Y. Polysaccharide-Based Edible Films/Coatings for the Preservation of Meat and Fish Products: Emphasis on Incorporation of Lipid-Based Nanosystems Loaded with Bioactive Compounds. *Foods* **2023**, *12*, 3268. [CrossRef] [PubMed]
63. Song, Q.; Jiang, L.; Yang, X.; Huang, L.; Yu, Y.; Yu, Q.; Chen, Y.; Xie, J. Physicochemical and functional properties of a water-soluble polysaccharide extracted from Mung bean (*Vigna radiate* L.) and its antioxidant activity. *Int. J. Biol. Macromol.* **2019**, *138*, 874–880. [CrossRef]
64. Bouaziz, F.; Koubaa, M.; Ben Jeddou, K.; Kallel, F.; Boisset Helbert, C.; Khelfa, A.; Ellouz Ghorbel, R.; Ellouz Chaabouni, S. Water-soluble polysaccharides and hemicelluloses from almond gum: Functional and prebiotic properties. *Int. J. Biol. Macromol.* **2016**, *93 Pt A*, 359–368. [CrossRef]
65. Shen, S.-G.; Lin, Y.-H.; Zhao, D.-X.; Wu, Y.-K.; Yan, R.-R.; Zhao, H.-B.; Tan, Z.-L.; Jia, S.-R.; Han, P.-P. Comparisons of Functional Properties of Polysaccharides from *Nostoc flagelliforme* under Three Culture Conditions. *Polymers* **2019**, *11*, 263. [CrossRef]
66. Spinei, M.; Oroian, M. Structural, functional and physicochemical properties of pectin from grape pomace as affected by different extraction techniques. *Int. J. Biol. Macromol.* **2023**, *224*, 739–753. [CrossRef] [PubMed]
67. Romdhane, M.B.; Haddar, A.; Ghazala, I.; Jeddou, K.B.; Helbert, C.B.; Ellouz-Chaabouni, S. Optimization of polysaccharides extraction from watermelon rinds: Structure, functional and biological activities. *Food Chem.* **2017**, *216*, 355–364. [CrossRef]
68. Chen, G.; Fang, C.; Chen, X.; Wang, Z.; Liu, M.; Kan, J. High-pressure ultrasonic-assisted extraction of polysaccharides from Mentha haplocalyx: Structure, functional and biological activities. *Ind. Crops Prod.* **2019**, *130*, 273–284. [CrossRef]
69. Jeddou, K.B.; Chaari, F.; Maktouf, S.; Nouri-Ellouz, O.; Helbert, C.B.; Ghorbel, R.E. Structural, functional, and antioxidant properties of water-soluble polysaccharides from potatoes peels. *Food Chem.* **2016**, *205*, 97–105. [CrossRef]
70. He, W.; Xiao, N.; Zhao, Y.; Yao, Y.; Xu, M.; Du, H.; Wu, N.; Tu, Y. Effect of polysaccharides on the functional properties of egg white protein: A review. *J. Food Sci.* **2021**, *86*, 656–666. [CrossRef]
71. Sharifian-Nejad, M.S.; Shekarchizadeh, H. Physicochemical and functional properties of oleaster (*Elaeagnus angustifolia* L.) polysaccharides extracted under optimal conditions. *Int. J. Biol. Macromol.* **2019**, *124*, 946–954. [CrossRef]
72. Gheribi, R.; Habibi, Y.; Khwaldia, K. Prickly pear peels as a valuable resource of added-value polysaccharide: Study of structural, functional and film forming properties. *Int. J. Biol. Macromol.* **2019**, *126*, 238–245. [CrossRef] [PubMed]
73. Adamiak, K.; Sionkowska, A. State of Innovation in Alginate-Based Materials. *Mar. Drugs* **2023**, *21*, 353. [CrossRef] [PubMed]
74. Meher, J.G.; Yadav, N.P.; Sahu, J.J.; Sinha, P. Determination of required hydrophilic-lipophilic balance of citronella oil and development of stable cream formulation. *Drug Dev. Ind. Pharm.* **2013**, *39*, 1540–1546. [CrossRef]
75. Mittal, N.; Mattu, P.; Kaur, G. Extraction and derivatization of *Leucaena leucocephala* (Lam.) galactomannan: Optimization and characterization. *Int. J. Biol. Macromol.* **2016**, *92*, 831–841. [CrossRef] [PubMed]

76. Bogdan, C.; Moldovan, M.L.; Man, I.M.; Crișan, M. Preliminary study on the development of an antistretch marks water-in-oil cream: Ultrasound assessment, texture analysis, and sensory analysis. *Clin. Cosmet. Investig. Dermatol.* **2016**, *9*, 249–255. [CrossRef]
77. Tasić-Kostov, M.; Arsić, I.; Pavlović, D.; Stojanović, S.; Najman, S.; Naumović, S.; Tadić, V. Towards a modern approach to traditional use: In vitro and in vivo evaluation of Alchemilla vulgaris L. gel wound healing potential. *J. Ethnopharmacol.* **2019**, *238*, 111789. [CrossRef]
78. Shin, G.H.; Chung, S.K.; Kim, J.T.; Joung, H.J.; Park, H.J. Preparation of chitosan-coated nanoliposomes for improving the mucoadhesive property of curcumin using the ethanol injection method. *J. Agric. Food Chem.* **2013**, *61*, 11119–11126. [CrossRef]
79. Haugstad, K.E.; Håti, A.G.; Nordgård, C.T.; Adl, P.S.; Maurstad, G.; Sletmoen, M.; Draget, K.I.; Dias, R.S.; Stokke, B.T. Direct Determination of Chitosan–Mucin Interactions Using a Single-Molecule Strategy: Comparison to Alginate–Mucin Interactions. *Polymers* **2015**, *7*, 161–185. [CrossRef]
80. Golshani, S.; Vatanara, A.; Amin, M. Recent Advances in Oral Mucoadhesive Drug Delivery. *J. Pharm. Pharm. Sci.* **2022**, *25*, 201–217. [CrossRef]
81. Puri, V.; Sharma, A.; Maman, P.; Rathore, N.; Singh, I. Overview of mucoadhesive biopolymers for buccal drug delivery systems. *Int. J. Appl. Pharm.* **2019**, *11*, 10–22159. [CrossRef]
82. Freitas, A.R.; Ribeiro, A.J.; Ribeiro, A.B.; Collado-Gonzalez, M.D.M.; Silva, L.R.; Alves, L.; Melro, E.; Antunes, F.E.; Veiga, F.; Morais, A.I.S.; et al. Modification of chicha gum: Antibacterial activity, ex vivo mucoadhesion, antioxidant activity and cellular viability. *Int. J. Biol. Macromol.* **2023**, *228*, 594–603. [CrossRef] [PubMed]
83. Özdemir, O.; Kopac, T. Cytotoxicity and biocompatibility of root canal sealers: A review on recent studies. *J. Appl. Biomater. Funct. Mater.* **2022**, *20*, 22808000221076325. [CrossRef] [PubMed]
84. Bhatia, S.K.; Yetter, A.B. Correlation of visual in vitro cytotoxicity ratings of biomaterials with quantitative in vitro cell viability measurements. *Cell Biol. Toxicol.* **2008**, *24*, 315–319. [CrossRef] [PubMed]
85. Stang, K.; Krajewski, S.; Neumann, B.; Kurz, J.; Post, M.; Stoppelkamp, S.; Fennrich, S.; Avci-Adali, M.; Armbruster, D.; Schlensak, C.; et al. Hemocompatibility testing according to ISO 10993-4: Discrimination between pyrogen- and device-induced hemostatic activation. *Mater. Sci. Eng. C Mater. Biol. Appl.* **2014**, *42*, 422–428. [CrossRef] [PubMed]
86. Nalezinková, M. In vitro hemocompatibility testing of medical devices. *Thromb. Res.* **2020**, *195*, 146–150. [CrossRef]
87. Srichamroen, A. Effect of extracted malva nut gum on reducing high glucose levels by Caco-2 cells. *Food Biosci.* **2018**, *21*, 107–116. [CrossRef]